


Volume 68, March 2013 ISSN 0010-938X



CORROSION SCIENCE

The Journal on Environmental Degradation of Materials and its Control
Editor-in-Chief: G. T. BURSTEIN, University of Cambridge, U.K.
An Official Journal of the Institute of Corrosion

CONTENTS

S. M. ABD EL HALHEM, S. ABD EL WANES, E. E. ABD EL AAL and A. FAROUK	1
E. E. ABD EL AAL, S. ABD EL WANES, A. FAROUK and S. M. ABD EL HALHEM	14
W. J. LI, M. C. YOUNG, C. L. LAI, W. KAI and L. W. TSIAY	25
J. A. DEWY and T. J. MARROW	34
W. SCHULZ, M. NOFF, M. FEIGL, I. DORFEL, R. SALDAN NEUMANN and A. KRANZMANN	44
M. FINSGAR	51
J. WANG, L.-K. WU, J.-H. ZHOU, J.-M. HU, J.-Q. ZHANG and C.-N. CAO	57
A. SAMANIEGO, I. LLORENTE and S. FERRI JR.	66
M. RINCON ORTIZ, M. A. RODRIGUEZ, R. M. CARRANZA and R. B. REBAK	72
C. A. DELLA ROVERE, F. S. SANTOS, R. SILVA, C. A. C. SOUZA and S. E. KURI	84
R. SANCHEZ-TOVAR, M. T. MONTANES and J. GARCIA-ANTON	91
S. LI and J. FU	101
A. MADHISHA	111

1 Factors affecting the corrosion behaviour of aluminium in acid solutions. I. Nitrogen and/or sulphur-containing organic compounds as corrosion inhibitors for Al in HCl solution
14 Factors affecting the corrosion behaviour of aluminium in acid solutions. II. Inorganic additives as corrosion inhibitors for Al in HCl solution
25 The effects of rolling and sensitization treatments on the stress corrosion cracking of 304L stainless steel in salt-spray environment
34 In situ observation of short fatigue crack propagation in oxygenated water at elevated temperature and pressure
44 Corrosion of uncoated and alumina coated steel X20CrMoV12-1 in H₂O-CO₂-O₂ and air at 600 °C
51 Galvanic series of different stainless steels and copper- and aluminium-based materials in acid solutions
57 Construction of a novel painting system using electrodeposited SiO₂ film as the pretreatment layer
66 Combined effect of composition and surface condition on corrosion behaviour of magnesium alloys AZ31 and AZ61
72 Oxyanions as inhibitors of chloride-induced crevice corrosion of Alloy 22
84 Influence of long-term low-temperature aging on the microhardness and corrosion properties of duplex stainless steel
91 Contribution of the flowing conditions to the galvanic corrosion of the copper/AISI 316L coupling in highly concentrated LiBr solutions
101 Improvement in corrosion protection properties of TiO₂ coatings by chromium doping
111 An amendment to the classical model of internal oxidation: Model-inherent transition characteristics

Contents continued on outside back cover
<http://www.elsevier.com/locate/corsci>

This article appeared in a journal published by Elsevier. The attached copy is furnished to the author for internal non-commercial research and education use, including for instruction at the authors institution and sharing with colleagues.

Other uses, including reproduction and distribution, or selling or licensing copies, or posting to personal, institutional or third party websites are prohibited.

In most cases authors are permitted to post their version of the article (e.g. in Word or Tex form) to their personal website or institutional repository. Authors requiring further information regarding Elsevier's archiving and manuscript policies are encouraged to visit:

<http://www.elsevier.com/copyright>



Contents lists available at SciVerse ScienceDirect

Corrosion Science

journal homepage: www.elsevier.com/locate/corsci

Oxyanions as inhibitors of chloride-induced crevice corrosion of Alloy 22

M. Rincón Ortíz^{a,c}, M.A. Rodríguez^{a,c,*}, R.M. Carranza^a, R.B. Rebak^b^aGerencia Materiales, Comisión Nacional de Energía Atómica, Instituto Sabato, UNSAM/CNEA, Av. Gral. Paz 1499, San Martín, B1650KNA Buenos Aires, Argentina^bGE Global Research, 1 Research Circle, Schenectady, NY 12309, USA^cCONICET, Instituto Sabato, UNSAM / CNEA, Gerencia Materiales, Comisión Nacional de Energía Atómica, B1650KNA, Buenos Aires, Argentina

ARTICLE INFO

Article history:

Received 9 May 2012

Accepted 31 October 2012

Available online 10 November 2012

Keywords:

- A. Alloy
- B. Polarization
- C. Crevice corrosion
- C. Repassivation

ABSTRACT

Oxyanions were tested as inhibitors of the chloride-induced crevice corrosion of Alloy 22, at 90 °C. Nitrate was the most efficient inhibitor showing $R_{CRIT} = 0.2$ for the two tested chloride concentrations. Sulphate showed R_{CRIT} values of 1 and 2 in 0.1 mol/L and 1 mol/L NaCl solutions, respectively. Carbonate showed $R_{CRIT} = 1$ while bicarbonate and carbonic acid did not show any inhibiting effect. Chromate and molybdate showed $R_{CRIT} = 0.5$ in 0.1 mol/L NaCl solutions being less effective in 1 mol/L NaCl solutions. Tungstate produced a repassivation potential increase without reaching a complete inhibition.

© 2012 Elsevier Ltd. All rights reserved.

1. Introduction

Crevice corrosion is a form of localised corrosion that may occur in occluded metallic surfaces where a stagnant solution is developed [1]. Pitting corrosion and crevice corrosion are essentially the same phenomena from an electrochemical viewpoint, although there are geometrical differences between them [2,3]. Chromium containing stainless steels and nickel alloys may suffer crevice corrosion when in contact with chloride containing solutions [1,4,5]. Ni–Cr–Mo alloys such as Alloy 22 are resistant to pitting corrosion but they may be prone to crevice corrosion in aggressive environmental conditions. Chloride is the main aggressive species causing crevice corrosion of Ni–Cr–Mo alloys in industrial applications. The crevice corrosion susceptibility of the alloys is increased at higher temperatures and higher chloride concentrations [6–8].

Certain species are able to mitigate or avoid the occurrence of localised attack. Crevice corrosion inhibitors may be commonly found in service environments or added on purpose to the environment. Crevice corrosion may occur only if the corrosion potential of the alloy (E_{CORR}) is higher than its repassivation potential ($E_{R,CREV}$) in the field conditions [6–8]. Cathodic inhibitors cause a shift of E_{CORR} to more active potentials, while anodic inhibitors cause a shift of $E_{R,CREV}$ to more noble potentials. There is practically no published research on cathodic inhibitors of the chloride-induced crevice corrosion of Alloy 22. On the other hand, there is considerable research dealing with anodic inhibitors of the chloride-induced crevice corrosion of Alloy 22. Nitrate, sulphate, carbonate, fluoride,

hydroxyl, organic acids and phosphate mitigate or inhibit crevice corrosion when added in sufficient amounts [9–20]. The inhibitor to chloride concentration ratio (R) is an important parameter. R is defined in Eq. (1) as the quotient of the inhibitor and chloride molar concentrations. There is a critical concentration ratio (R_{CRIT}) above which inhibition is complete. R_{CRIT} is the lowest R value at which crevice corrosion is not observed [21].

$$R = \frac{[Inhibitor]}{[Cl^-]} \quad (1)$$

Chloride-induced crevice corrosion occurs due to the formation of hydrochloric acid solution in the creviced region [2,3]. Anodic inhibitors act by avoiding the development of hydrochloric acid or by hampering its deleterious action. Rebak [21] proposed four different modes in which an anodic inhibitor of the chloride-induced crevice corrosion of Alloy 22 may act:

1. Stabilisation of the Cr₂O₃-rich passive film by maintaining an oxidizing environment within the crevice.
2. Reduction of the inhibitor to a lower oxidation state along with protons consumption.
3. Reduction of the general corrosion rate in the creviced area.
4. Sequestration of protons released by the hydrochloric acid due to a lower dissociation constant of the corresponding acid.

The effective inhibitors should act by many of these proposed modes at the same time, while the less effective inhibitors act by one or two of these modes [21]. However, these four modes of inhibition are not independent from each other. For instance, a reduction of the general corrosion rate of the alloy (mode 3) may result

* Corresponding author. Tel.: +54 11 6772 7353; fax: +54 11 6772 7362.

E-mail addresses: maalrodr@cnea.gov.ar, martinrz@gmail.com (M.A. Rodríguez).

from an inhibitor consuming or sequestering protons (mode 4); an oxidizing environment (mode 1) is generated by an inhibitor which may reduce to a lower oxidation state (mode 2).

The objective of the present work is to gain further insight regarding the mechanisms of crevice corrosion inhibition of Alloy 22. The localised acidification model is used to explain the different effects of anodic inhibitors on $E_{R,CREV}$.

2. Theoretical background

The localised acidification model assumes that pitting and crevice corrosion result from the local acidification caused by cation hydrolysis [2]. The excess of cations within the pit/crevice causes the migration of anions towards the alloy surface under the influence of an electric field. Migration of chlorides leads to an even lower pH since the activity coefficient of proton increases with chloride concentration [1]. According to this model, localised corrosion will be stable when the product of the diffusion path (x) and the anodic current density (i) is higher than a critical ($CRIT$) value (Eq. (2)).

$$xi > (xi)_{CRIT} \quad (2)$$

In crevice corrosion testing the diffusion path depends on the crevice geometry, which is determined by the crevice formers type and materials, applied torque, surface roughness, etc. Consequently, x may be considered constant provided that all these parameters are the same in all the tests. Under these conditions, Eq. (2) becomes Eq. (3), where i_{CRIT} is the anodic current density above which crevice corrosion is stabilised.

$$i > i_{CRIT} \quad (3)$$

The crevice corrosion repassivation potential is the sum of three contributions as stated in Eq. (4). E_{CORR}^* is the corrosion potential of the alloy in the local solution, η is the polarisation needed for sustaining the critical chemistry (Eqs. (2) and), and $\Delta\Phi$ is the ohmic drop within the crevice [2].

$$E_{R,CREV} = E_{CORR}^* + \eta + \Delta\Phi \quad (4)$$

An anodic crevice corrosion inhibitor must produce an increase of $E_{R,CREV}$ by increasing one or more of the three contributions (E_{CORR}^* , η and $\Delta\Phi$).

3. Experimental method

The specimens were prepared from wrought mill annealed plate stock. The chemical composition of Alloy 22 in weight percent was 59.20% Ni, 20.62% Cr, 13.91% Mo, 2.68% W, 2.80% Fe, 0.01% Co, 0.14% Mn, 0.002% C, and 0.0001% S. Prism Crevice Assembly (PCA) specimens were used [22]. They are shown in Fig. 1. The crevicing mechanism contains 24 artificially creviced spots formed by two ceramic washers (crevice formers) wrapped with a 70 μ m-thick PTFE tape. A torque of 5 N·m was applied to the system formed by the two crevice formers sandwiching the specimen as shown in Fig. 1. The torque was applied by a screw bolt and nut system made of titanium. The bolt was electrically isolated from the Alloy 22 specimen by a thick PTFE tape. The crevicing mechanism and the material type of crevice formers are of main importance in crevice corrosion testing. The present device is the most efficient for obtaining reproducible and conservative repassivation potentials [23,24]. The tested surface area was approximately 14 cm². The specimens had a finished grinding of abrasive paper number 600 and were degreased in acetone and washed in distilled water within the hour prior to testing.

All the electrochemical tests were conducted in a one-liter, three-electrode vessel (ASTM G 5) [25]. Nitrogen (N₂) was purged

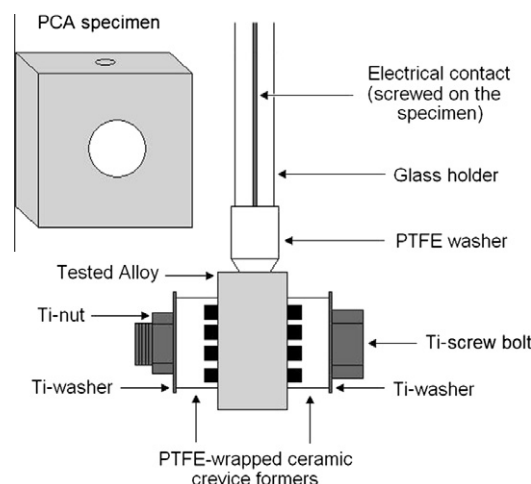


Fig. 1. Drawing of the Prism Crevice Assembly (PCA) specimen configuration.

through the solution 1 h prior to testing and was continued throughout the entire test. A water-cooled condenser combined with a water trap was used to avoid evaporation of the solution and to prevent the ingress of air (oxygen). The temperature of the solution was controlled by immersing the cell in a water bath, which was kept at a constant temperature. The set point temperature was 90 °C. All the tests were performed at ambient pressure. The reference electrode was a saturated calomel electrode (SCE), which has a potential of 0.242 V more positive than the standard hydrogen electrode (SHE). The reference electrode was connected to the solution through a water-cooled Luggin probe and it was kept at room temperature. The electrode potentials were not corrected for the thermal liquid junction potential since it was assumed to be on the order of a few mV. The counter electrode consisted in a flag of platinum foil (total area 50 cm²) spot-welded to a platinum wire. All the potentials in this paper are reported in the SCE scale.

The crevice corrosion repassivation potential was determined by the Potentiodynamic–Galvanostatic–Potentiodynamic (PD–GS–PD) method [17]. This is a modification of the Tsujikawa–Hisamatsu electrochemical (THE) method (ASTM G 192) [22]. The PD–GS–PD method has been recently validated for Alloy 22 [23,26]. It consists of three stages: (1) a potentiodynamic polarisation (at a scan rate of 0.167 mV/s) in the anodic direction up to reaching an anodic current of 30 μ A, (2) the application of a constant anodic current of $I_{GS} = 30 \mu$ A (approximately $i_{GS} = 2 \mu$ A/cm²) for 2 h, and (3) a potentiodynamic polarisation (at 0.167 mV/s) in the cathodic direction, from the previous potential up to reaching alloy repassivation. The parameter obtained from this technique is a cross-over potential (E_{CO}) determined at the intersection of the forward (stage 1) and reverse (stage 3) scans. At least three repetitions were performed for each test condition to obtain an average value. The specimens remained at the open circuit potential for 15 min before the PD–GS–PD test started.

The testing solutions were 0.1 mol/L NaCl and 1 mol/L NaCl solutions plus the addition of different concentrations of inhibitors. Tested inhibitors included the oxyanions nitrate, sulphate, carbonate, chromate, molybdate and tungstate. Table 1 shows the oxyanion salts used along with the corresponding values of R and solution pH. Sodium salts were used. Carbonate, bicarbonate and carbonic acid solutions were obtained from sodium bicarbonate solution. The pH values corresponding to the maximum concentration of carbonate, bicarbonate and carbonic acid at 90 °C are 11.5, 7 and 3, respectively [27]. The pH was adjusted by additions of small volumes of NaOH and HCl to obtain the desired value. Nitrate,

Table 1
Oxyanion salts used in the present work along with the corresponding values of *R* and solution pH.

Oxyanion salts	$R = [\text{Inhibitor}]/[\text{Cl}^-]$	pH
Nitrate: NaNO ₃	0.01–0.5	5.5–6.5
Sulphate: Na ₂ SO ₄	0.1–2	5.5–6.6
Carbonic acid: H ₂ CO ₃ *	0.01–1	3.0
Bicarbonate: NaHCO ₃	0.01–2	7.0
Carbonate: Na ₂ CO ₃ **	0.01–2	11.5
Chromate: Na ₂ CrO ₄	0.01–1	6.5–8.0
Molybdate: Na ₂ MoO ₄	0.01–1	5.5–7.5
Tungstate: Na ₂ WO ₄	0.1–2	6.8–11.0

* Prepared as NaHCO₃ and pH adjusted with HCl.

** Prepared as NaHCO₃ and pH adjusted with NaOH.

sulphate, chromate, molybdate and tungstate were tested at the solution pH determined by the hydrolysis of the corresponding oxyanion at the given concentration. The pH of tungstate solutions increased significantly with the tungstate concentration. The hydrolysis of the other tested oxyanions led to pH changes of less than 2 units.

Potentiodynamic polarisation curves were performed using uncreviced specimens of Alloy 22, in some of the previously described solutions. The scan rate was 0.167 mV/s.

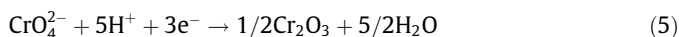
All the specimens were examined after testing with a light optical microscope and some of them were observed in the scanning electron microscope (SEM).

4. Results

4.1. Potentiodynamic polarisation curves

Fig. 2 shows polarisation curves of Alloy 22 in 1 mol/L NaCl solutions and with the addition of different inhibitors. The polarisation curves showed a wide passive range followed by a current increase. An anodic peak followed by a current decrease was observed in the presence of bicarbonate, carbonate, chromate, molybdate and tungstate (curves in solutions containing bicarbonate, molybdate and tungstate are not shown). This anodic peak was neither observed in pure chloride solutions nor in chloride plus sulphate solutions. The anodic peak shifted to lower potentials and showed the highest current density in the presence of carbonate and bicarbonate. A constant passive current density ranging from 0.5 to 1 μA/cm² was observed in all the tests with the exception of the chromate-containing solution. In the latter, Alloy 22 showed the lowest passive current density which slowly increased

with the applied potential (Fig. 2). This may be attributed to the superposition of the cathodic current from the reduction of CrO₄²⁻ to Cr₂O₃ thus decreasing the net measured current. CrO₄²⁻ may reduce to Cr₂O₃ according to Eq. (5) [28]. The positive slope in the passive range may be due to film thickening caused by the Cr₂O₃ deposition. A thicker film may also produce a decrease of the cathodic current of CrO₄²⁻ reduction (Fig. 2).



The anodic current density selected for stage 2 of the PD–GS–PD method (*i*_{CS} = 2 μA/cm²) was three times higher than the average passive current density (Fig. 2). This low current value is higher than the passive current but not so high to produce significant transpassive dissolution that could lead to misleading repassivation potentials.

4.2. Crevice corrosion

4.2.1. Repassivation potential

Fig. 3 shows PD–GS–PD tests on Alloy 22 in 1 mol/L NaCl + NaNO₃ solutions at different *R* values. The three stages of the PD–GS–PD tests are observed in Fig. 3. This technique provides a cross-over potential (*E*_{CO}) which is determined at the intersection of the forward (stage 1) and reverse (stage 3) scans. When there was no cross-over between the forward and the reverse scans, *E*_{CO} was determined at the intersection of the reverse scan and the extrapolation of the passive current in the forward scan at higher potentials. The potential drop in the galvanostatic step was associated with crevice corrosion initiation (*R* = 0.02 and *R* = 0.1 in Fig. 3). *E*_{CO} increased as *R* increased. The potential drop during the galvanostatic step was negligible for *R* = 0.2 suggesting crevice corrosion did not occur, which was verified by optical microscopy and SEM at high magnification. The potential increased during the galvanostatic step at *R* = 0.5 and there was no crossover between the forward and reverse potential scans (Fig. 3). In these cases, *E*_{CO} was determined at the intersection of the extrapolation of the passive current at higher potentials and the reverse scan.

Figs. 4–8 show *E*_{CO} of Alloy 22 as a function of *R* in the different solutions. The symbols are average values and the error bars represent one standard deviation calculated from at least three tests. Fig. 4 shows *E*_{CO} of Alloy 22 as a function of *R* in chloride plus nitrate and chloride plus sulphate solutions. In chloride plus nitrate solutions *E*_{CO} increased slightly between *R* = 0.01 and *R* = 0.1, and it increased significantly from *R* = 0.1 to *R* = 0.2. For 1 mol/L and 0.1 mol/L NaCl solutions containing nitrate the value of *R*_{CRIT} was

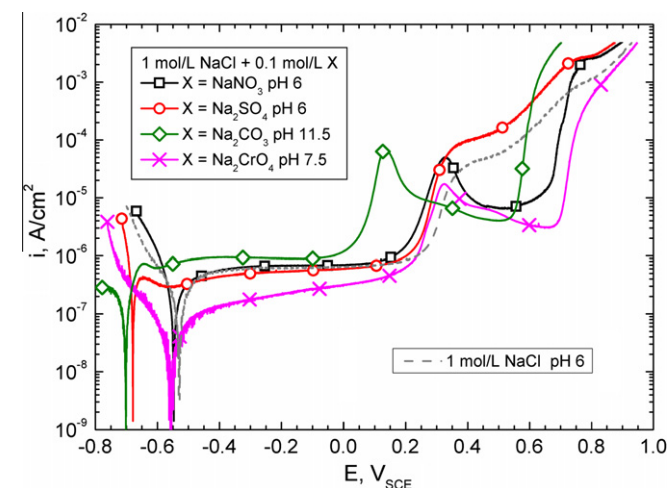


Fig. 2. Potentiodynamic polarisation curves of Alloy 22 in 1 mol/L NaCl solutions and with the addition of different inhibitors, at 90 °C.

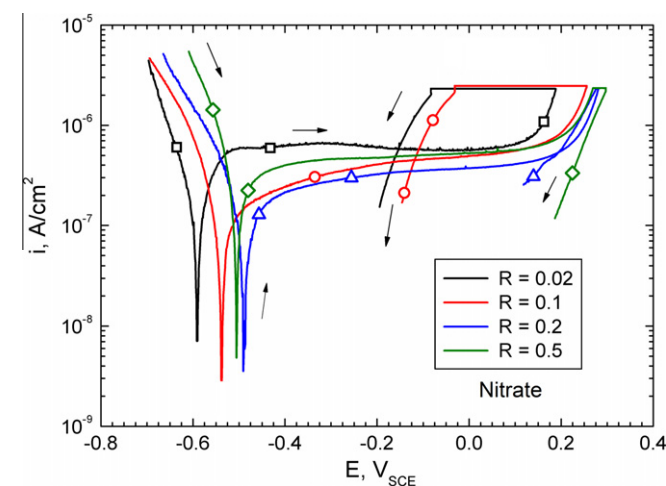


Fig. 3. PD–GS–PD tests on Alloy 22 in 1 mol/L NaCl + NaNO₃ solutions, at 90 °C.

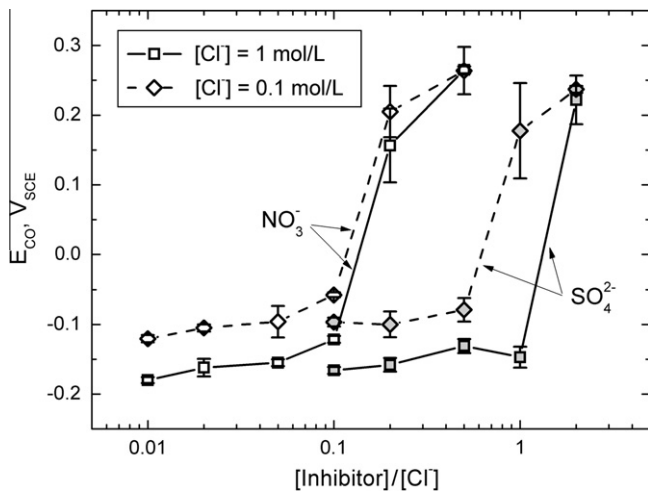


Fig. 4. Cross over potential from PD-GS-PD tests as a function of the inhibitor to chloride concentration ratio for Alloy 22. Symbols are average values and error bars represent one standard deviation.

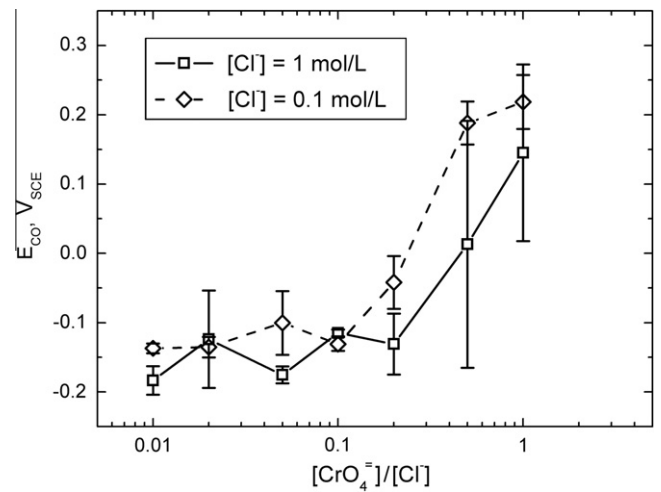


Fig. 7. Cross over potential from PD-GS-PD tests as a function of the chromate to chloride concentration ratio for Alloy 22. Symbols are average values and error bars represent one standard deviation.

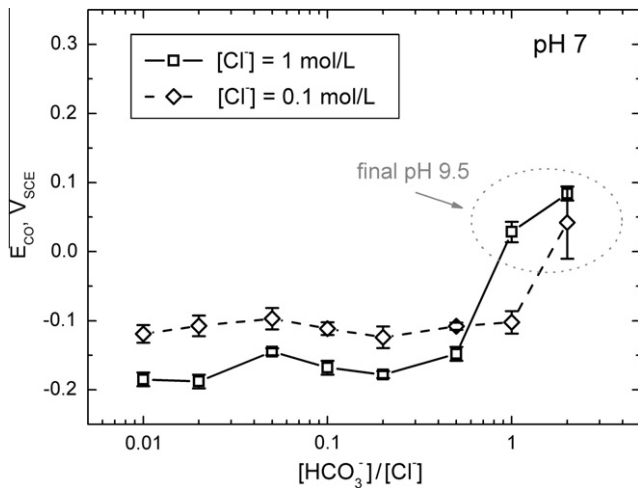


Fig. 5. Cross over potential from PD-GS-PD tests as a function of the bicarbonate to chloride concentration ratio for Alloy 22. Symbols are average values and error bars represent one standard deviation.

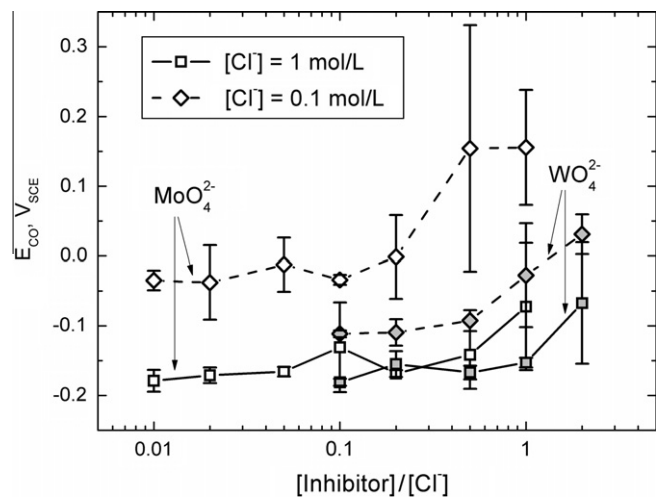


Fig. 8. Cross over potential from PD-GS-PD tests as a function of the inhibitor to chloride concentration ratio for Alloy 22. Symbols are average values and error bars represent one standard deviation.

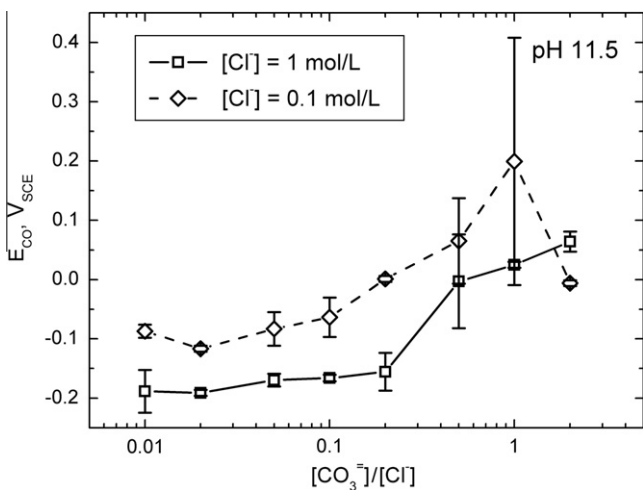


Fig. 6. Cross over potential from PD-GS-PD tests as a function of the carbonate to chloride concentration ratio for Alloy 22. Symbols are average values and error bars represent one standard deviation.

determined to be 0.2 ($R_{CRIT} = 0.2$). The scatter of the E_{CO} results was higher at R_{CRIT} . The absence of crevice corrosion at R_{CRIT} was verified by optical microscopy observation in all the cases. In chloride plus sulphate solutions, $R_{CRIT} = 1$ was observed in the 0.1 mol/L NaCl and $R_{CRIT} = 2$ in the 1 mol/L NaCl solutions. E_{CO} did not show a significant increase with R below R_{CRIT} .

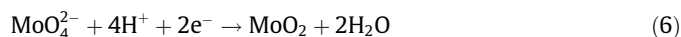
Carbonic acid, bicarbonate and carbonate were tested as inhibitors of the chloride-induced crevice corrosion. The solution pH was set at 3 (carbonic acid), 7 (bicarbonate) and 11.5 (carbonate) in order to determine the effectiveness of the different species of this chemical equilibrium. Carbonic acid did not produce any E_{CO} increase of Alloy 22 neither when tested at R values up to 0.5 in 1 mol/L NaCl nor when tested at R values up to 1 in 0.1 mol/L NaCl solutions (not shown). Figs. 5 and 6 show E_{CO} of Alloy 22 as a function of R in chloride solutions with additions of bicarbonate and carbonate, respectively. E_{CO} remained constant as R increased in bicarbonate solutions, in a wide range of R values (Fig. 5). An increase of E_{CO} was observed in some tests at $R = 1$ and $R = 2$, in bicarbonate solutions. However, a pH increase up to 9.5 was detected after these tests indicating a high concentration of carbonate in solution. At $R = 1$, the 0.1 mol/L NaCl solution seemed to be more

aggressive than the 1 mol/L NaCl solution (Fig. 5). This behaviour resulted from the pH increase observed during the test in the 1 mol/L NaCl solution which did not occur in the 0.1 mol/L NaCl solution. The increase in E_{CO} observed in Fig. 5 was attributed to the presence of significant amounts of carbonate. E_{CO} showed an increase as R increased in carbonate solutions (Fig. 6). For both the 1 mol/L and 0.1 mol/L NaCl solutions containing carbonate it was determined that $R_{CRIT} = 1$. A large scatter of the results was observed at $R = 0.5$ and particularly at $R = 1$, in 0.1 mol/L NaCl. A drop of E_{CO} was observed at $R = 2$, in 0.1 mol/L NaCl solutions. This drop in E_{CO} was not associated to a higher crevice corrosion susceptibility of the alloy at $R = 2$, but with a particular feature of the PD–GS–PD technique as will be discussed later.

Fig. 7 shows E_{CO} of Alloy 22 as a function of R in chloride plus chromate solutions. The R_{CRIT} was 0.5 in the 0.1 mol/L NaCl and $R_{CRIT} = 1$ in the 1 mol/L NaCl solutions. E_{CO} showed a wide scatter in 1 mol/L NaCl solutions. The determination of the cross-over potential in chromate solutions was muddled by the superposition of the cathodic current from the reduction of CrO_4^{2-} to Cr_2O_3 (Fig. 2), as discussed above. This cathodic current increased as the chromate concentration increased, thus decreasing the net current in the passive range which affected the cross over between the forward and the reverse scans. Moreover, Cr_2O_3 was likely to be deposited on the alloy surface as a result of CrO_4^{2-} reduction. This deposition may have also affected the determination of E_{CO} .

Fig. 8 shows E_{CO} of Alloy 22 as a function of R in chloride plus molybdate and chloride plus tungstate solutions. In the molybdate containing solutions, large differences (of approximately 0.15 V) were found among E_{CO} in 1 mol/L and 0.1 mol/L NaCl solutions. $R_{CRIT} = 0.5$ was found for molybdate in 0.1 mol/L NaCl solutions. Complete crevice corrosion inhibition was not attained in the 1 mol/L NaCl solutions with molybdate and E_{CO} only showed a

slight increase at $R = 1$. A wide scatter of E_{CO} was observed at certain R values. The scatter may be an effect of molybdate reduction as in the case of chromate. MoO_4^{2-} may reduce to MoO_2 according to Eq. (6) [28].



In chloride plus tungstate solutions, complete crevice corrosion inhibition was not reached at any tested R value (Fig. 8). Testing at higher R values was not possible because of the lack of solubility of the tungsten salt. E_{CO} showed only a slight increase above $R = 1$.

Fig. 9 shows SEM images of Alloy 22 specimens after PD–GS–PD tests in different solutions. Figs. 9(a, b, and d) show crevice corroded specimens tested in chloride solutions with nitrate, sulphate and chromate additions, respectively, at $R < R_{CRIT}$. Corrosion products were observed covering the attacked areas. Some alloy grains and twins were discernible. This type of attack is called crystalline [7]. The localised attack did not penetrate deep into the alloy. This may be either a consequence of the low applied current in the galvanostatic step (stage 2) or it may be related to the inhibition of the alloy dissolution by insoluble molybdates (coming from the alloy elements) which cover the alloy surface and force the propagation to shift to areas unprotected by these layers [29]. Fig. 9(d) shows a specimen tested in chloride plus chromate solutions. Preferential attack at triple points was observed as reported by Jakupi et al. [30]. Fig. 9(c) shows a specimen tested in a chloride plus carbonate solution, at $R > R_{CRIT}$. No crevice corrosion was observed below the crevice former tooth.

Figs. 4–8 indicate that E_{CO} generally increased as R increased from the lowest tested R to R_{CRIT} . E_{CO} showed a sharp increase at R_{CRIT} . The cross over potential was not an actual repassivation potential above R_{CRIT} since crevice corrosion did not occur

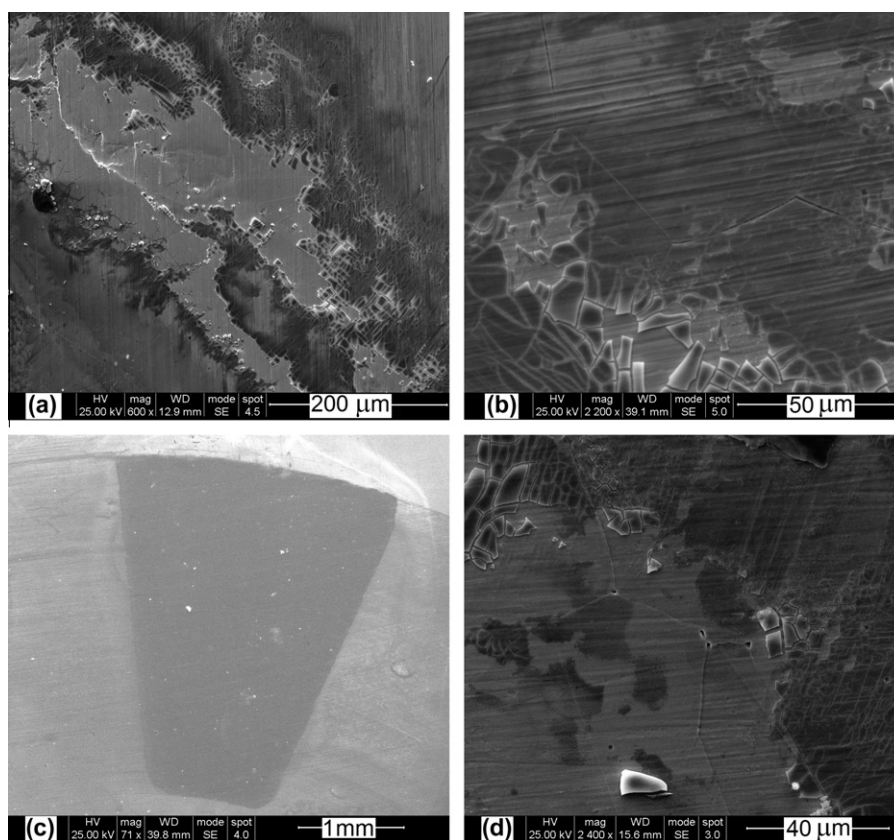


Fig. 9. SEM images of Alloy 22 specimens after PD–GS–PD tests in (a) 1 mol/L NaCl + 0.1 mol/L $NaNO_3$, (b) 0.1 mol/L NaCl + 0.05 mol/L Na_2SO_4 , (c) 0.1 mol/L NaCl + 0.1 mol/L Na_2CO_3 and (d) 0.1 mol/L NaCl + 0.005 mol/L Na_2CrO_4 solutions, at 90 °C.

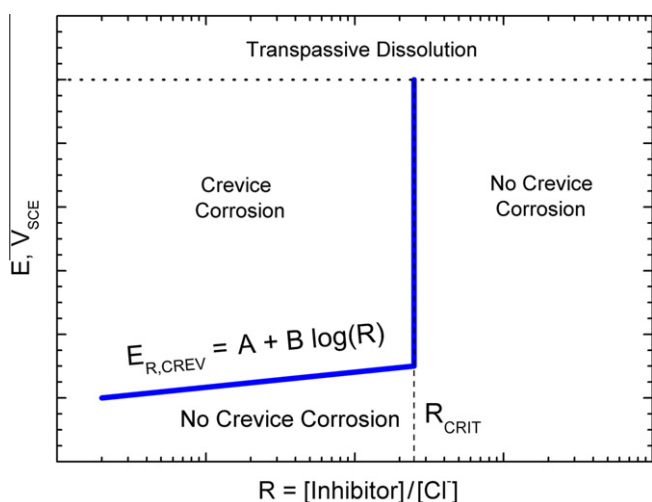


Fig. 10. Schematic $E_{R,CREV}$ vs. R diagram for Alloy 22 in a chloride plus inhibitor solution indicating areas of corrosion and areas of protection.

(Fig. 3). Therefore, the equality $E_{R,CREV} = E_{CO}$ only holds at $R < R_{CRIT}$. Above R_{CRIT} , E_{CO} was associated with the onset of transpassivity. Fig. 10 shows a schematic representation of $E_{R,CREV}$ vs. R for Alloy 22 in a chloride solution containing an inhibitor. Below R_{CRIT} , the relationship shown in Eq. (7) is generally observed, where A and B are constants [31]. Eq. (7) was fitted to the experimental data below R_{CRIT} , for all the tested inhibitors. The vertical line in Fig. 10 shows the value of R_{CRIT} . Alloy 22 is susceptible to crevice corrosion below R_{CRIT} and above $E_{R,CREV}$. Alloy 22 may suffer transpassive dissolution above an applied potential which depends on solution pH and the considered inhibitor (Fig. 10).

$$E_{R,CREV} = A + B \log(R) \quad (7)$$

Figs. 11 and 12 show $E_{R,CREV}$ as a function of R for Alloy 22 in 0.1 mol/L NaCl and 1 mol/L NaCl solutions plus different inhibitors. The vertical line showing R_{CRIT} in Figs. 11 and 12 was drawn from the corresponding $E_{R,CREV}$ to the onset of transpassivity, which was determined as E_{CO} in the tests where no crevice corrosion occurred. $E_{R,CREV}$ in the absence of inhibitors (pure NaCl solutions) is also plotted for comparison. The efficiency of inhibitors may be charac-

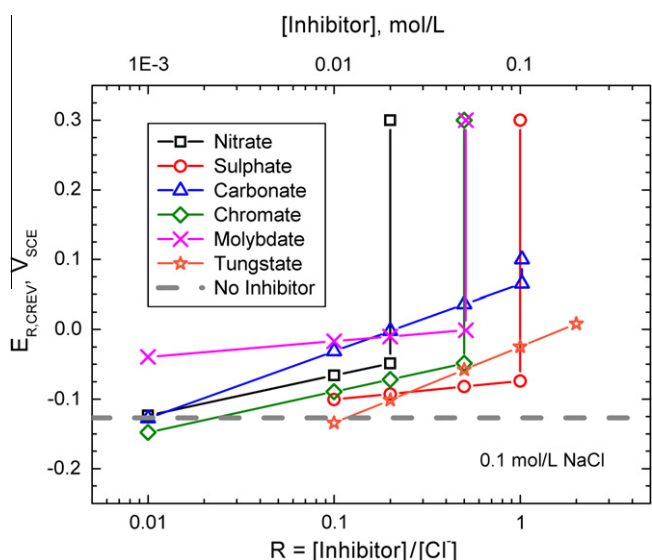


Fig. 11. Repassivation potential as a function of R for Alloy 22 in 0.1 mol/L NaCl solutions plus different inhibitors, at 90 °C.

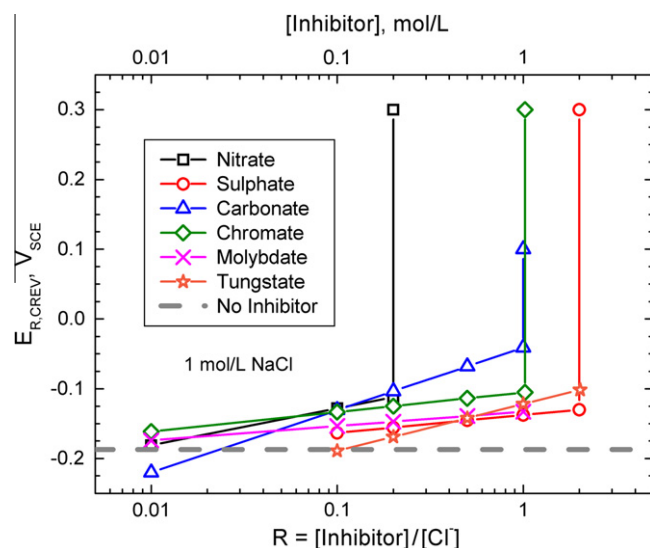


Fig. 12. Repassivation potential as a function of R for Alloy 22 in 1 mol/L NaCl solutions plus different inhibitors, at 90 °C.

terised mainly by R_{CRIT} and in a lesser extent by the slope (B) of Eq. (7). R_{CRIT} and B obtained in the present work in 1 mol/L NaCl and 0.1 mol/L NaCl solutions are listed in Table 3. The lower R_{CRIT} and the higher B the more effective the inhibitor was. Nitrate showed the lowest R_{CRIT} among tested inhibitors and a high B value. Chromate and molybdate showed a low R_{CRIT} in 0.1 mol/L NaCl, but they were less effective as inhibitors in 1 mol/L NaCl. Molybdate was unable to completely inhibit crevice corrosion in the latter solution. Carbonate showed $R_{CRIT} = 1$ and a high B both in 0.1 mol/L NaCl and 1 mol/L NaCl solutions. Sulphate showed a high R_{CRIT} and a low B in the tested solutions. Tungstate showed a high B but it was unable to inhibit crevice corrosion. Carbonic acid and bicarbonate were not considered in this discussion since they did not show R_{CRIT} and their B was close to zero.

4.2.2. Potential transient during the galvanostatic step

In certain conditions, crevice corrosion inhibitors may delay the initiation of the localised attack without affecting significantly $E_{R,CREV}$. Analyses of this effect may render valuable information regarding the mechanism by which the inhibitors act. The time dependent effects of the tested inhibitors were analysed by comparing the potential transients during the 2-h galvanostatic hold of PD-GS-PD tests in chloride plus inhibitor solutions. The applied anodic current in all the tests was $30 \mu\text{A}$ (approximately $2 \mu\text{A}/\text{cm}^2$). Figs. 13–19 show the potential transients in some of the tested solutions. A single transient for each tested condition is shown since it was considered to be representative of the many repetitions performed. The transient corresponding to a PD-GS-PD test in 1 mol/L or 0.1 mol/L NaCl solutions at pH 6 is shown for comparison. Crevice corrosion initiation was usually associated with a potential drop in the 2-h long galvanostatic step. A constant potential as a function of time generally indicated absence of crevice corrosion.

Fig. 13 shows the potential transients in 0.1 mol/L NaCl + NaNO_3 solutions. In the pure 0.1 mol/L NaCl solution the potential started to drop immediately when the galvanostatic current was applied to the specimen, suggesting that the crevice corrosion initiated without induction time. Crevice corrosion initiation was delayed as R increased for $R > 0.01$. When R increased from 0.02 to 0.1 the initiation time increased and the final potential at 2-h treatment also slightly increased suggesting the beneficial effect of adding nitrate to values even below R_{CRIT} . A constant potential of

Table 2
Literature review of R_{CRIT} for the oxyanions tested in the present work in different experimental conditions.

Reference	Metallurgical condition	Temperature, °C	Oxyanion	$[Cl^-]$, mol/L	R_{CRIT}
Dunn et al. [10,14]	As welded	95	Nitrate	0.1	0.5
Dunn et al. [11,13]	Mill annealed 5 min. at 870 °C	80	Nitrate	8	0.1
		110	Nitrate	8	0.15
		80	Nitrate	8	0.1
		110	Nitrate	8	0.3
		95	Carbonate	0.5	0.05
		95	Bicarbonate	0.5	0.2
Mishra and Frankel [17]	Mill annealed	90	Nitrate	1–4	0.2
			Sulphate	0.1	0.8
			Sulphate	1	1.5

Table 3
Slope (B) of Eq. (7) ($E_{R,CREV} = A + B \log(R)$) and critical inhibitor to chloride ratio (R_{CRIT}) for the tested species.

Species	B, mV/dec.	R_{CRIT}		
		$[Cl^-] = 0.1$ mol/L	$[Cl^-] = 1$ mol/L	
NO_3^-	58	53	0.2	0.2
SO_4^{2-}	27	26	1	2
CO_3^{2-}	96	90	1	1
CrO_4^{2-}	58	28	0.5	1
MoO_4^{2-}	23	21	0.5	-
WO_4^{2-}	110	67	-	-

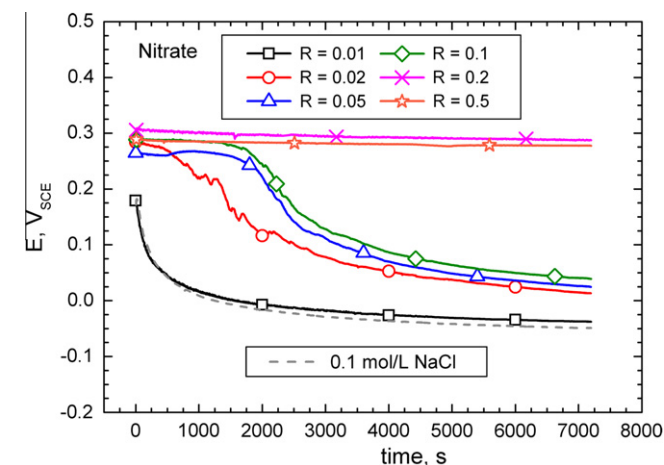


Fig. 13. Potential transients during the galvanostatic step of PD-GS-PD tests ($i_{CS} = 2 \mu A/cm^2$) on Alloy 22 in 0.1 mol/L NaCl + NaNO₃ solutions, at 90 °C.

approximately $0.3 V_{SCE}$ was observed at $R = 0.2$ and $R = 0.5$, suggesting complete inhibition from the onset, that is, crevice corrosion never initiated. Fig. 14 shows the potential transients in 1 mol/L NaCl + Na₂SO₄ solutions. For values of R from 0 to 0.2 crevice corrosion initiated in the first 10 min of treatment but as the amount of sulphate increased the final potential after the 2-h treatment increased. A pronounced delay of crevice corrosion initiation was observed at $R = 0.5$ and $R = 1$. The potential remained approximately at $0.3 V_{SCE}$ in the test at $R = 2$, where crevice corrosion did not occur (similarly as the values of potential in the case of nitrate solutions, Fig. 13).

Fig. 15 shows the potential transients in 1 mol/L NaCl + NaHCO₃ solutions. A minor potential increase was observed for $R = 0.5$, a delayed initiation of crevice corrosion was observed at $R = 1$, and a complete inhibition of crevice corrosion at $R = 2$. In the latter case, the potential remained approximately constant at $0.15 V_{SCE}$.

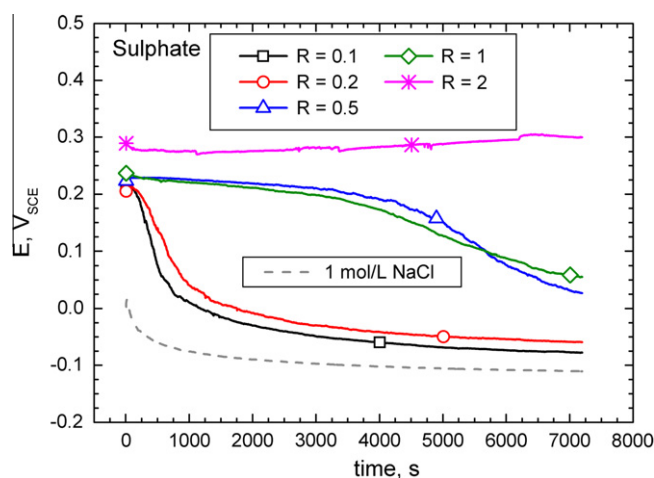


Fig. 14. Potential transients during the galvanostatic step of PDA-GS-PD tests ($i_{CS} = 2 \mu A/cm^2$) on Alloy 22 in 1 mol/L NaCl + Na₂SO₄ solutions, at 90 °C.

Fig. 16 shows the potential transients in 0.1 mol/L NaCl + Na₂CO₃ solutions. In the tests at $0.01 \leq R \leq 0.2$, the potential initially increased in time until it reached a maximum and then decreased. A continuous potential increase in time was observed at $R = 0.5$ and $R = 1$ (Fig. 16). The observed potential evolution in time was a consequence of the presence of an anodic peak at low potentials (Fig. 2). The potential increase may be attributed to transient processes related to the anodic peak, while the potential drop was indicative of the crevice corrosion initiation. Fig. 16 shows that the delay in the crevice corrosion initiation increased as R increased. After the 2-h galvanostatic polarisation, low potentials (between $0.0 V_{SCE}$ and $0.1 V_{SCE}$) were observed in tests at $R = 1$ and $R = 0.5$ (Fig. 16). These potentials correspond to the current peak observed in chloride plus carbonate solutions at low anodic potentials (Fig. 2). The occurrence of this peak resulted in a decrease of E_{CO} for $R > R_{CRIT}$ (Fig. 6) which did not imply a higher crevice corrosion susceptibility.

Fig. 17 shows the potential transients during the galvanostatic treatment in 1 mol/L NaCl + Na₂CrO₄ solutions. An apparent delay of crevice corrosion initiation was observed from $R = 0.01$ to $R = 0.2$. The transients in Fig. 17 show definitely that even small additions of chromate raise the potential during the galvanostatic step. The potential increased in time at $R = 0.5$ and $R = 1$ suggesting a complete crevice corrosion inhibition. However, crevice corrosion was observed in some specimens after the tests at $R = 0.5$ (Fig. 7). The potential after the 2-h galvanostatic polarisation was higher for the chromate containing 1 mol/L NaCl solutions when compared to the pure 1 mol/L NaCl solution (Fig. 17). This effect could be attributed to the high concentration of chromate. The reduction of CrO_4^{2-} to Cr_2O_3 produced a larger polarisation to attain the same

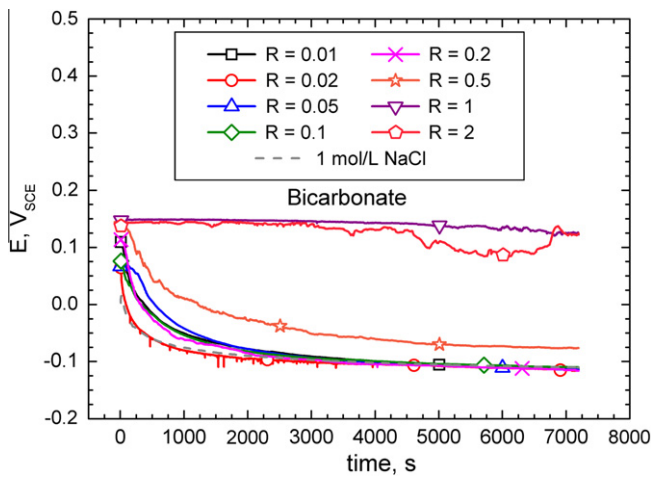


Fig. 15. Potential transients during the galvanostatic step of PD-GS-PD tests ($i_{CS} = 2 \mu\text{A}/\text{cm}^2$) on Alloy 22 in 1 mol/L NaCl + NaHCO₃ solutions, at 90 °C.

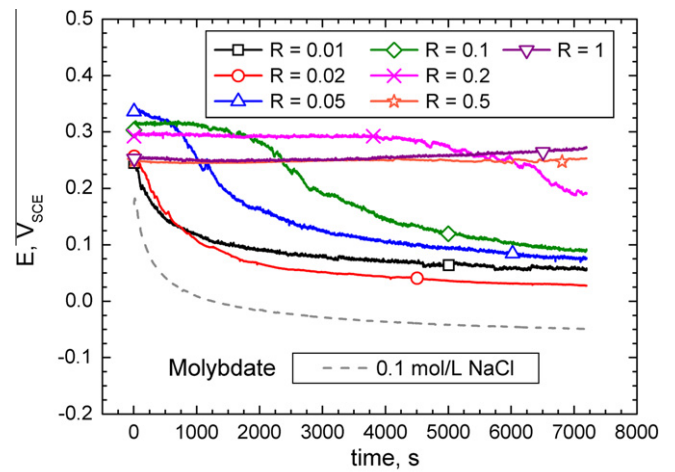


Fig. 18. Potential transients during the galvanostatic step of PD-GS-PD tests ($i_{CS} = 2 \mu\text{A}/\text{cm}^2$) on Alloy 22 in 0.1 mol/L NaCl + Na₂MoO₄ solutions, at 90 °C.

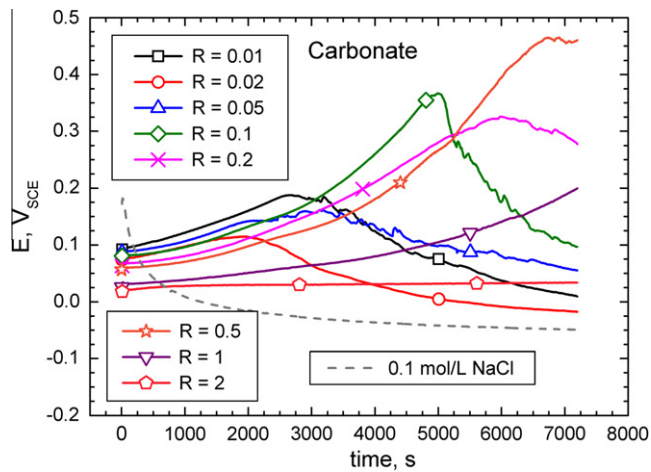


Fig. 16. Potential transients during the galvanostatic step of PD-GS-PD tests ($i_{CS} = 2 \mu\text{A}/\text{cm}^2$) on Alloy 22 in 0.1 mol/L NaCl + Na₂CO₃ solutions, at 90 °C.

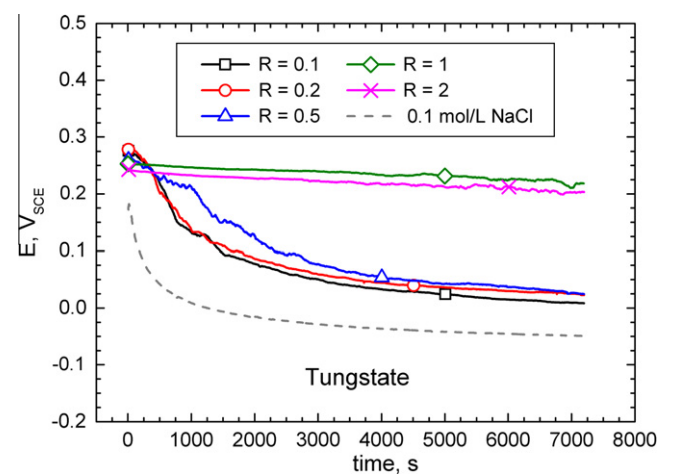


Fig. 19. Potential transients during the galvanostatic step of PD-GS-PD tests ($i_{CS} = 2 \mu\text{A}/\text{cm}^2$) on Alloy 22 in 0.1 mol/L NaCl + Na₂WO₄ solutions, at 90 °C.

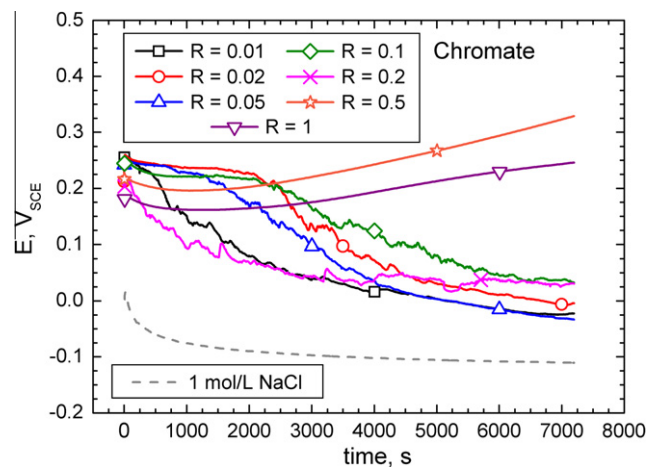


Fig. 17. Potential transients during the galvanostatic step of PD-GS-PD tests ($i_{CS} = 2 \mu\text{A}/\text{cm}^2$) on Alloy 22 in 1 mol/L NaCl + Na₂CrO₄ solutions, at 90 °C.

net anodic current in the galvanostatic step. Furthermore, Cr₂O₃ may have been deposited on the alloy surface due to CrO₄²⁻ reduction according to Eq. (5), thus producing a thicker and more protective film.

Fig. 18 shows the potential transients in 0.1 mol/L NaCl + Na₂MoO₄ solutions. Crevice corrosion initiation was gradually delayed as R increased. Also the potential at the end of the 2-h treatment increased as R increased from 0 to 0.2. The potential remained constant at approximately 0.25 V_{SCE} for $R = 0.5$ and $R = 1$ indicating the complete inhibition of crevice corrosion as reported before (Fig. 8). Fig. 19 shows the potential transients in 0.1 mol/L NaCl + Na₂WO₄ solutions. Even smaller additions of tungstate for R values of 0.1 to 0.5 increased the potential from the baseline value in pure NaCl ($R = 0$). The potential remained almost constant at 0.25 V_{SCE} for $R = 0.5$ and $R = 1$; however, crevice corrosion was observed in the specimens after all the tests even for R values 0.1 and 2 (Fig. 8).

5. Discussion

5.1. Nitrate

Nitrate is a well-known inhibitor of the chloride-induced pitting corrosion of stainless alloys [32–40]. Nitrate retards pitting nucleation, reduces the propagation rates of metastable pitting and reduces the current density of stable pitting propagation [39]. Nitrate addition causes an increase of the pitting potential and the appearance of an inhibition potential above which the stainless steels passivate. In this way, nitrate acts both at low and at high

potentials, reducing the potential range of pitting corrosion occurrence. Nitrate inhibition at high potentials does not apply for crevice corrosion since the potential drop within the crevice leads to regions of lower potentials where localised corrosion can proceed [3,31,35,37]. Consequently, the proposed mechanisms for the passivation of growing pits above the inhibition potential cannot be considered in the present case of crevice corrosion as explained elsewhere [3,31].

In the present work, nitrate was the best inhibitor among the tested species. It showed the lowest R_{CRIT} along with a high B value (Table 3). The efficiency of nitrate as a crevice corrosion inhibitor depended on R . Nitrate showed $R_{CRIT} = 0.2$ and a similar B value in 0.1 mol/L and 1 mol/L chloride solutions. These results of R_{CRIT} are consistent with those informed in the literature (Table 2) [9–14,17]. The inhibiting effects of nitrate observed in the present work may be attributed to the reduction of nitrate to elemental nitrogen via Eq. (8) [28]. The reduction of 1 mol of nitrates consumes 6 mol of protons thus increasing the local pH. Reduction of nitrates to nitrogen is a likely reaction within stainless steels pits [38] and it has been confirmed in aluminium pits [41]. Elemental nitrogen may block preferential dissolution sites on the surface (active kinks) [36].



As a crevice corrosion inhibitor of Alloy 22, nitrate is able to act in the four different modes proposed by Rebak [21]. However, its main effect is likely to be the pH increase caused by its reduction [12]. This mechanism is consistent with the low R_{CRIT} and the high B value determined in the present work (Table 3). Present results showed that below R_{CRIT} , nitrate delayed crevice corrosion initiation and produced an increase of $E_{R,CREV}$ (Figs. 4 and 13). These effects may be also attributed to proton consumption. Acidic nitrate (nitric acid) may also passivate the active crevice by enhancing the formation of Cr_2O_3 [42].

5.2. Sulphate

Sulphate has been extensively studied as an inhibitor of pitting corrosion of stainless steels [37,38,43–46]. Sulphate may enhance pitting corrosion when present in small amounts along with chloride [43]. Sulphate cannot be reduced within an acidic solution and it is stable as SO_4^{2-} or HSO_4^- . Several researchers postulate that sulphate acts mainly by a supporting electrolyte effect. This mechanism involves the competitive migration and adsorption of sulphate and chloride on the alloy surface [37,38,44,45]. Sulphate accumulates preferentially at the alloy/solution interface by migration due to its higher charge with respect to chloride, which prevents the increase of chloride concentration above a critical value. [2]. Sulphate reduces the solubility of the metal cations produced by dissolution within the pits [46]. Alloy passivation may occur below precipitated sulphate films by inward diffusion of water [36]. pH buffering within the local solution is postulated since the second dissociation constant of sulphuric acid has a low value [21,37].

In the present work, sulphate showed a high R_{CRIT} along with a low slope B . Its effectiveness as inhibitor decreased as the chloride concentration increased (Table 3). The obtained R_{CRIT} values are close to those informed by Mishra and Frankel [17] under similar experimental conditions (Table 2). Ilevbare [15] reports tests on MA Alloy 22 in 4 mol/L NaCl + Na_2SO_4 ($R = 0.01$ and 0.1) at temperatures from 45 to 105 °C. No crevice corrosion is observed at 45 °C. At 60 °C, sulphate produces an increase of $E_{R,CREV}$. At 75 °C and higher temperatures, less severe localised attack is observed in the presence of sulphate. However, an increase of $E_{R,CREV}$ is not reported [15]. Dunn et al. [11,13] report that sulphate causes the

increase of $E_{R,CREV}$ of thermally aged (5 min. at 870 °C) Alloy 22 in 0.5 mol/L NaCl ($R = 0.5$), at 95 °C. The works of Ilevbare and Dunn et al. do not report a value for R_{CRIT} since complete crevice corrosion inhibition was not observed. These authors used R values below the R_{CRIT} determined in the present work; therefore, the present results are consistent with their findings.

Present results showed that sulphate was able to delay crevice corrosion initiation of Alloy 22 without producing an increase of $E_{R,CREV}$, below R_{CRIT} (Fig. 14). Sulphate may act in the modes 3 and 4 proposed by Rebak [21]. However, a pH buffering effect is very limited since H_2SO_4 is a strong acid. In the conditions tested in the present work, sulphate is likely to act by a supporting electrolyte mechanism enhanced by its double electrical charge. The observed delay and the eventual inhibition of crevice corrosion may have been the results of the preferential accumulation of sulphate over chloride within the crevice. That is, less chloride is able to concentrate in the creviced area with the presence of sulphate.

5.3. Carbonate, bicarbonate and carbonic acid

Few studies are reported on the inhibiting effects of carbonate, bicarbonate and carbonic acid on the pitting corrosion of stainless steels. Anions of weak inorganic acids are generally localised corrosion inhibitors. These acids hamper or make it more difficult the development of a critical chemistry within a pit due to pH buffering [2]. The crevice corrosion of 254 SMO stainless steel in 4% NaCl at 70 °C is completely inhibited with the addition of 0.5 mol/L NaHCO_3 [45]. The pitting potential of 316L stainless steel increases with the concentration of bicarbonate in a 0.5 mol/L NaCl solution [47]. Dunn et al. [11,13] studied the effects of carbonate and bicarbonate on crevice corrosion of thermally aged (5 min. at 870 °C) Alloy 22, in 0.5 mol/L NaCl, at 95 °C. They report $R_{CRIT} = 0.05$ for carbonate and $R_{CRIT} = 0.2$ for bicarbonate, suggesting that carbonate is a crevice corrosion inhibitor as effective as nitrate. However, they do not report the value of the pH of the solution.

In the present work, carbonate was the only species of this chemical equilibrium that showed an inhibiting effect under the tested conditions. Bicarbonate and carbonic acid neither inhibited crevice corrosion nor produced a significant $E_{R,CREV}$ increase of Alloy 22 in the tested conditions. Above pH 11.5, carbonate is the main species of the equilibrium, but its concentration relative to bicarbonate becomes important at pH >9 [27]. In pure chloride solutions, the repassivation potential of Alloy 22 remains constant in the pH range from 2 to 12 [48]. Therefore, the observed inhibitive effect cannot be attributed to hydroxyl but to carbonate. Present results indicated that the bulk pH became an important variable in the presence of the carbonate/bicarbonate equilibrium. The differences between the present results and those reported by Dunn et al. [11,13] may be attributed to the different crevice formers, metallurgical conditions of the alloy and/or the solution pH.

In the present work, carbonate showed $R_{CRIT} = 1$ and a high B value independently of the chloride concentration studied (Table 3). Carbonate also delayed crevice corrosion initiation below R_{CRIT} (Fig. 16). Carbonate may act in the modes 3 and 4 proposed by Rebak [21]. A gradual effect of carbonate as R increased is in agreement with an inhibition mechanism based on pH buffering. Carbonate may also preferentially accumulate within the crevice due to its double electrical charge in a similar inhibiting fashion as sulphate; that is allowing for less of detrimental chloride accumulation. However, carbonate may become bicarbonate as long as the pH decreases. Present results showed that bicarbonate was unable to inhibit crevice corrosion of Alloy 22 under the tested conditions (Fig. 5). Bicarbonate might inhibit crevice corrosion at lower chloride concentrations as in the case of fluoride [16]. Carbonic acid is unable to migrate since it is not a charged species and it cannot take protons. Consequently, carbonic acid cannot decrease

significantly local acidification and chloride accumulation within the crevice.

5.4. Chromate, molybdate and tungstate

Chromate, molybdate and tungstate may change the ionic selectivity of the passive film from anion selective to cation selective, preventing the ingress of chloride ions [49]. Cr, Mo and W are present as alloying elements in Alloy 22. The oxidizing power of the species decreases as $\text{CrO}_4^{2-} > \text{MoO}_4^{2-} > \text{WO}_4^{2-}$ [28]. Chromate and molybdate may reduce to oxides consuming protons according to Eq. 5 and 6, respectively [28]. The reduced cations, Cr^{3+} and Mo^{4+} , may accumulate inside the film [39,50–52] or form dense precipitates with an ohmic blocking action. These precipitates may be preferentially deposited at the more reactive sites of the metal surface physically hampering further metal dissolution [35,53,54]. Furthermore, reactions 5 and 6 cause a decrease of the local acidity affecting the transition from nucleation to metastable pitting [37,53]. Molybdate forms polymeric species, such as $\text{Mo}_7\text{O}_{24}^{6-}$ and $\text{Mo}_8\text{O}_{26}^{4-}$, at pH <6. Polymerisation involves proton consumption [37,44]. Molybdic acid (H_2MoO_4) may form and precipitate during localised corrosion propagation, leading to repassivation by the blocking of active sites. Polymeric molybdates have been observed in recent crevice corrosion studies on Alloy 22 [55]. Some authors suggest that molybdate in solution may have an inhibiting effect similar to that of molybdenum in the alloy [44,50,56] while others say that molybdate additions in solution do not fully account for the inhibiting effects of alloyed molybdenum [57,58]. Tungstate is less oxidizing than chromate and molybdate. Consequently, the reduction of tungstate to W_2O_5 or WO_2 is unlikely. WO_3 may precipitate consuming protons at low pH via Eq. (9). WO_3 may have a passivating or an ohmic blocking action similar to MoO_2 . Tungsten is passive at low pH [28].



In the present work, chromate and molybdate showed the same R_{CRIT} in 0.1 mol/L NaCl solutions (Table 3). Below R_{CRIT} , molybdate was more efficient than chromate since it led to higher $E_{\text{R,CREV}}$ (Fig. 11) and stronger delays in crevice corrosion initiation (Fig. 18). However, molybdate was unable to inhibit crevice corrosion in 1 mol/L NaCl while chromate was still effective in this higher chloride concentration (Table 3 and Fig. 12). Chromate and molybdate may act in the four different modes proposed by Rebak [21]. In the conditions tested in the present work, chromate and molybdate may have produced an oxidizing environment within the crevice reducing themselves with proton consumption (Eq. 5 and 6). The reduction products may have blocked further metal dissolution. Present results indicate that molybdate was not oxidizing in 1 mol/L NaCl solutions but it only acted by an ohmic effect blocker (Fig. 8). In these conditions, molybdate may act only in the modes 3 and 4 [21].

In the present work, tungstate delayed crevice corrosion initiation and produced an increase of $E_{\text{R,CREV}}$ at high R , but it was unable to completely inhibit crevice corrosion in the tested conditions (Figs. 8 and 19). Tungstate is able to act in the inhibiting modes 3 and 4 [21]. Tungstate was likely to act by an ohmic effect due to the precipitation of insoluble compounds (Eq. (9)). Inhibitors mainly based on ohmic effects are less effective for controlling crevice corrosion than for pitting corrosion since the former occurs at lower current densities [31].

5.5. Localised acidification model

Anodic inhibitors may increase $E_{\text{R,CREV}}$ at $R < R_{\text{CRIT}}$, avoid localised corrosion at $R \geq R_{\text{CRIT}}$ and/or delay the initiation of the attack.

Table 4

Terms of the Eq. (4), from the localised acidification model, that may be affected by the tested inhibitors.

Species	E_{CORR}^*	η	$\Delta\Phi$
NO_3^-	YES	YES	NO
SO_4^{2-}	NO	YES	NO
CO_3^{2-}	NO	YES	NO
CrO_4^{2-}	YES	YES	YES
MoO_4^{2-}	YES	YES	YES
WO_4^{2-}	NO	NO	YES

The localised acidification model accounts for the increase of $E_{\text{R,CREV}}$ due to the increase of any of the contributions stated in Eq. (4) (E_{CORR}^* , η and $\Delta\Phi$) [2]. The model also accounts for complete inhibition of localised corrosion when the conditions stated in Eq. (2) are not satisfied. However, this is a steady state model and it does not account for delaying effects.

E_{CORR}^* may increase in the presence of oxidising inhibitors. This possibility needs to be verified by measurements in HCl plus inhibitor solutions. η may increase in the presence of inhibitors due to an increase of i_{CRIT} or due to an increase of the anodic Tafel slope. Anions of weak acids produce an increase of i_{CRIT} [2]. Anions acting by the supporting electrolyte effect may produce an increase of the anodic Tafel slope. $\Delta\Phi$ increases in the presence of inhibitors producing a resistive salt film on the alloy surface.

Table 4 shows the terms of the Eq. (4) affected by the inhibitors tested in the present work. Nitrate is an oxidising species in acidic conditions which may cause an E_{CORR}^* increase. The proton consumption caused by nitrate reduction (Eq. (8)) should lead to an increase of η since a higher polarisation is needed to reach i_{CRIT} . Sulphate may cause an increase of η since it acts by the supporting electrolyte effect [37,38,44,45]. A higher polarisation is needed for reaching i_{CRIT} in the presence of sulphate. Carbonate may cause an increase of η by the supporting electrolyte and the pH buffering effects. i_{CRIT} and the Tafel slope may increase in the presence of carbonate. Chromate and molybdate are oxidising species which may be reduced with proton consumption (Eq. 5 and 6) [37,53]. The reaction products are oxides which may be passivating or having an ohmic blocking action [35,53,54]. Reduction of chromate produces Cr_2O_3 which is the main component of the passive film (Eq. (5)). Reduction of molybdate may cause precipitation of polymerised oxides which may increase the ohmic drop [37,44]. Chromate and molybdate may cause an increase of E_{CORR}^* , η and $\Delta\Phi$. In concentrated chloride solutions, molybdate seemed to be less oxidising and its effect may be reduced to an increase of $\Delta\Phi$ (Fig. 8). Tungstate may act by precipitation of WO_3 which have an ohmic blocking action leading to an increase of $\Delta\Phi$ (Eq. (9)).

The mechanisms by which the tested inhibitors acted have been discussed. However, the preceding description is still qualitative. A higher number of mechanisms involved in the inhibition may not be necessarily indicative of a higher efficiency of the considered inhibitor. For instance, nitrate was more efficient than chromate and molybdate in spite of affecting probably only two contributions in Eq. (4). A quantitative assessment of the considered mechanisms is still needed to account for the observed effectiveness of the inhibitors.

6. Conclusions

Inhibitors of the chloride-induced crevice corrosion of Alloy 22 were tested in 0.1 mol/L and 1 mol/L NaCl solutions, at 90 °C. Nitrate was the most efficient among the tested inhibitors showing $R_{\text{CRIT}} = 0.2$ regardless the chloride concentration. Sulphate showed $R_{\text{CRIT}} = 1$ in 0.1 mol/L NaCl solutions and $R_{\text{CRIT}} = 2$ in 1 mol/L NaCl solutions. Carbonate showed $R_{\text{CRIT}} = 1$ regardless the chloride

concentration. Bicarbonate and carbonic acid did not show any inhibiting effect on crevice corrosion of Alloy 22 under the tested conditions. Chromate and molybdate showed $R_{CRIT} = 0.5$ in 0.1 mol/L NaCl solutions. Chromate showed $R_{CRIT} = 1$ in 1 mol/L NaCl solutions while molybdate was unable to completely inhibit crevice corrosion at 1 mol/L chloride concentration. Tungstate was unable to completely inhibit crevice corrosion but it produced an significant $E_{R,CREV}$ increase in the tested conditions.

Acknowledgements

Financial support from the Agencia Nacional de Promoción Científica y Tecnológica of the Ministerio de Ciencia, Tecnología e Innovación Productiva from Argentina and from the Universidad Nacional de San Martín is acknowledged.

References

- [1] Z. Szklarska-Smialowska, Pitting and Crevice Corrosion, NACE International, Houston, TX, USA, 2005.
- [2] J.R. Galvele, Transport processes and the mechanism of pitting of metals, *J. Electrochem. Soc.* 123 (1976) 464–474.
- [3] J.R. Galvele, Tafel's law in pitting corrosion and crevice corrosion susceptibility, *Corros. Sci.* 47 (2005) 3053–3067.
- [4] R.B. Rebak, Corrosion and environmental degradation, in: R.W. Cahn, P. Haasen, E.J. Kramer (Eds.), *Material Science and Engineering: A Comprehensive Treatment*, vol. II, Wiley-VCH, Weinheim, Germany, 2000.
- [5] D.C. Agarwal, N. Sridhar, Nickel and nickel alloys, in: *Uhlrig's Corrosion Handbook*, John Wiley & Sons Inc., 2011, pp. 837–852.
- [6] R.M. Carranza, The crevice corrosion of Alloy 22 in the Yucca Mountain nuclear waste repository, *JOM* (2008) 58–65.
- [7] R.B. Rebak, Factors affecting the crevice corrosion susceptibility of Alloy 22 Paper No. 05610, in: *Corrosion 2005*, NACE International, Houston, TX, USA, 2005, pp. 1–17.
- [8] G.M. Gordon, Speller award lecture: corrosion considerations related to permanent disposal of high-level radioactive waste, *Corrosion* 58 (2002) 811–825.
- [9] B.A. Kehler, G.O. Ilevbare, J.R. Scully, Crevice corrosion stabilization and repassivation behavior of Alloy 625 and Alloy 22, *Corrosion* 57 (2001) 1042–1065.
- [10] D.S. Dunn, C.S. Brossia, Assessment of passive and localized corrosion processes for Alloy 22 as a high-level nuclear waste container material Paper No. 02548, in: *Corrosion 2002*, NACE International, Houston, TX, USA, 2002, pp. 1–13.
- [11] D.S. Dunn, L. Yang, C. Wu, G.A. Cragnolino, Effect of inhibiting oxyanions on the localized corrosion susceptibility of waste package container materials, *Scientific Basis for Nuclear Waste Management XXVIII*, vol. 824, Materials Research Society, Boston, MA, USA, 2004, pp. CC1.7.1–CC1.7.6.
- [12] G.O. Ilevbare, K.J. King, S.R. Gordon, H.A. Elayat, G.E. Gdowski, T.S.E. Gdowski, Effect of nitrate on the repassivation potential of Alloy 22 in chloride-containing environments, *J. Electrochem. Soc.* 152 (2005) B547–B554.
- [13] D. Dunn, Y. Pan, K.-T. Chiang, L. Yang, G.A. Cragnolino, X. He, The localized corrosion resistance and mechanical properties of Alloy 22 waste package outer containers, *JOM* 57 (2005) 49–55.
- [14] D.S. Dunn, Y.-M. Pan, L. Yang, G.A. Cragnolino, Localized corrosion susceptibility of Alloy 22 in chloride solutions: part 2 – effect of fabrication processes, *Corrosion* 62 (2006) 3–12.
- [15] G.O. Ilevbare, Effect of sulfate on the passive and crevice corrosion properties of Alloy 22 in 4 M sodium chloride, *Corrosion* 62 (2006) 340–356.
- [16] R.M. Carranza, M.A. Rodríguez, R.B. Rebak, Effect of fluoride ions on crevice corrosion and passive behavior of Alloy 22 in hot chloride solutions, *Corrosion* 63 (2007) 480–490.
- [17] A.K. Mishra, G.S. Frankel, Crevice corrosion repassivation of Alloy 22 in aggressive environments, *Corrosion* 64 (2008) 836–844.
- [18] R.M. Carranza, C.M. Giordano, M.A. Rodríguez, R.B. Rebak, Effect of organic acid additions on the general and localized corrosion susceptibility of Alloy 22 in chloride solutions Paper No. 08578, in: *Corrosion 2008*, NACE International, Houston, TX, USA, 2008, pp. 1–20.
- [19] R.M. Carranza, M. Rincón Ortíz, M.A. Rodríguez, R.B. Rebak, Corrosion resistance of Alloy 22 in chloride and silicate solutions, in: 14th International Conference on Environmental Degradation of Materials in Nuclear Power Systems – Water Reactors, American Nuclear Society, La Grange Park, IL, USA, 2009.
- [20] M. Miyagusuku, R.B. Rebak, R.M. Carranza, The effect of phosphate ions on corrosion behavior of Alloy 22 Paper No. 10238, in: *Corrosion 2010*, NACE International, Houston, TX, USA, 2010, pp. 1–10.
- [21] R.B. Rebak, Mechanisms of inhibition of crevice corrosion in Alloy 22, *Scientific Basis for Nuclear Waste Management XXX*, vol. 985, Materials Research Society, Boston, MA, USA, 2006, pp. 0985–NN08–04.
- [22] ASTM G192–08 Standard Test Method for Determining the Crevice Repassivation Potential of Corrosion-Resistant Alloys Using a Potentiodynamic-Galvanostatic-Potentiostatic Technique, 2006.
- [23] C.M. Giordano, M. Rincón Ortíz, M.A. Rodríguez, R.M. Carranza, R.B. Rebak, Crevice corrosion testing methods for measuring repassivation potential of Alloy 22, *Corros. Eng. Sci. Technol.* 46 (2011) 129–133.
- [24] X. Shan, J.H. Payer, Effect of polymer and ceramic crevice formers on the crevice corrosion of Ni–Cr–Mo Alloy 22, *Corrosion* 66 (2010). 105005–105005–14.
- [25] ASTM G5 – 94 (2011) e1 Standard Reference Test Method for Making Potentiostatic and Potentiodynamic Anodic Polarization Measurements, 2011.
- [26] M. Rincón Ortíz, M.A. Rodríguez, R.M. Carranza, R.B. Rebak, Determination of the crevice corrosion stabilization and repassivation potentials of a corrosion-resistant alloy, *Corrosion* 66 (2010) 105002–1–105002–12.
- [27] P.K. Shukla, D.S. Dunn, K.-T. Chiang, O. Pensado, Stress corrosion cracking model for Alloy 22 in the potential Yucca Mountain repository environment Paper No. 06502, in: *Corrosion 2006*, NACE International, Houston, TX, USA, 2006, pp. 1–25.
- [28] M. Pourbaix, *Atlas of Electrochemical Equilibria in Aqueous Solutions*, second ed., NACE International, Houston, TX, USA, 1974.
- [29] P. Jakupi, J.J. Noël, D.W. Shoesmith, The evolution of crevice corrosion damage on the Ni–Cr–Mo–W Alloy-22 determined by confocal laser scanning microscopy, *Corros. Sci.* 54 (2012) 260–269.
- [30] P. Jakupi, J.J. Noël, D.W. Shoesmith, Intergranular corrosion resistance of $\Sigma 3$ grain boundaries in Alloy 22, *Electrochem. Solid-State Lett.* 13 (2010) C1.
- [31] M.A. Rodríguez, Inhibition of localized corrosion in chromium containing stainless alloys, *Corros. Rev.* 30 (2012) 19–32.
- [32] W. Schwenk, Theory of stainless steel pitting, *Corrosion* 20 (1964) 129t–137t.
- [33] H.P. Leckie, H.H. Uhlig, Environmental factors affecting the critical potential for pitting in 18–8 stainless steel, *J. Electrochem. Soc.* 113 (1966) 1262.
- [34] I.L. Rosenfeld, I.S. Danilov, Electrochemical aspects of pitting corrosion, *Corros. Sci.* 7 (1967) 129–142.
- [35] R.C. Newman, M.A.A. Ajjawi, A micro-electrode study of the nitrate effect on pitting of stainless steels, *Corros. Sci.* 26 (1986) 1057–1063.
- [36] R.C. Newman, T. Shahabi, The effect of alloyed nitrogen or dissolved nitrate ions on the anodic behaviour of austenitic stainless steel in hydrochloric acid, *Corros. Sci.* 27 (1987) 827–838.
- [37] H. Yashiro, A. Oyama, K. Tanno, Effects of temperature and potential on the inhibitive action of oxoacid salts for pitting in high-temperature chloride solutions, *Corrosion* 53 (1997) 290–297.
- [38] C.S. Brossia, R.G. Kelly, Influence of alloy sulfur content and bulk electrolyte composition on crevice corrosion initiation of austenitic stainless steel, *Corrosion* 54 (1998) 145–154.
- [39] Y. Zuo, H. Wang, J. Zhao, J. Xiong, The effects of some anions on metastable pitting of 316L stainless steel, *Corros. Sci.* 44 (2002) 13–24.
- [40] R.S. Lillard, G. Vasquez, D.F. Bahr, The Kinetics of anodic dissolution and repassivation on stainless steel 304L in solutions containing nitrate, *J. Electrochem. Soc.* 158 (2011) C194–C201.
- [41] S.B. de Wexler, J.R. Galvele, Anodic behavior of aluminum straining and a mechanism for pitting, *J. Electrochem. Soc.* 121 (1974) 1271–1276.
- [42] J.J. Gray, J.R. Hayes, G.E. Gdowski, B.E. Viani, C.A. Orme, Influence of solution pH, anion concentration, and temperature on the corrosion properties of Alloy 22, *J. Electrochem. Soc.* 153 (2006) B61–B67.
- [43] G.A. Cragnolino, N. Sridhar, Localized corrosion of a candidate container material for high-level nuclear waste disposal, *Corrosion* 47 (1991) 464–472.
- [44] M. Ürgen, A.F. Çakir, The effect of molybdate ions on the temperature dependent pitting potential of austenitic stainless steels in neutral chloride solutions, *Corros. Sci.* 32 (1991) 835–852.
- [45] E.A. Abd El Meguid, A.A. Abd El Latif, Electrochemical and SEM study on Type 254 SMO stainless steel in chloride solutions, *Corros. Sci.* 46 (2004) 2431–2444.
- [46] P.C. Pistorius, G.T. Burstein, Growth of corrosion pits on stainless steel in chloride solution containing dilute sulphate, *Corros. Sci.* 33 (1992) 1885–1897.
- [47] J.-J. Park, S.-I. Pyun, W.-J. Lee, H.-P. Kim, Effect of bicarbonate ion additives on pitting corrosion of Type 316L stainless steel in aqueous 0.5 M sodium chloride solution, *Corrosion* 55 (1999) 380–387.
- [48] M.A. Rodríguez, R.M. Carranza, R.B. Rebak, Effect of potential on crevice corrosion kinetics of Alloy 22, *Corrosion* 66 (2010) 015007–1–015007–14.
- [49] M. Sakashita, N. Sato, Bipolar fixed charge induced passivity, in: R.P. Frankenthal, J. Kruger (Eds.), *Passivity of Metals: Proceedings of the Fourth International Symposium on Passivity*, The Electrochemical Society, Princeton, NJ, 1978, pp. 479–483.
- [50] K. Sugimoto, Y. Sawada, The role of alloyed molybdenum in austenitic stainless steels in the inhibition of pitting in neutral halide solutions, *Corrosion* 32 (1976) 347–352.
- [51] J. Gluszek, G.B. Freeman, J. Baron, J. Kubicki, Effect of composition modification of passive films formed on ferritic stainless steel on resistance to pitting, *Corrosion* 41 (1985) 527–532.
- [52] A. Devasenapathi, V.S. Raja, Effect of externally added molybdate on repassivation and stress corrosion cracking of Type 304 stainless steel in hydrochloric acid, *Corrosion* 52 (1996) 243–249.

- [53] G.O. Ilevbare, G.T. Burstein, The inhibition of pitting corrosion of stainless steels by chromate and molybdate ions, *Corros. Sci.* 45 (2003) 1545–1569.
- [54] J.N. Wanklyn, The role of molybdenum in the crevice corrosion of stainless steels, *Corros. Sci.* 21 (1981) 211–225.
- [55] P. Jakupi, F. Wang, J.J. Noël, D.W. Shoesmith, Corrosion product analysis on crevice corroded Alloy-22 specimens, *Corros. Sci.* 53 (2011) 1670–1679.
- [56] R.C. Newman, The dissolution and passivation kinetics of stainless alloys containing molybdenum-II. Dissolution kinetics in artificial pits, *Corros. Sci.* 25 (1985) 341–350.
- [57] R.S. Lillard, M.P. Jurinski, J.R. Scully, Crevice corrosion of Alloy 625 in chlorinated ASTM artificial ocean water, *Corrosion* 50 (1994) 251–265.
- [58] W.J. Tobler, S. Virtanen, Effect of Mo species on metastable pitting of Fe18Cr alloys – a current transient analysis, *Corros. Sci.* 48 (2006) 1585–1607.